

Spin Superfluid Josephson Phase Qubits

So Takei,^{1,2} Yaroslav Tserkovnyak,² and Masoud Mohseni³

¹*Department of Physics, Queens College of the City University of New York, Queens, NY 11367, USA*

²*Department of Physics and Astronomy, University of California, Los Angeles, CA 90095, USA*

³*Google Research, Venice, CA 90291, USA*

(Dated: December 16, 2015)

A proposal for a macroscopic solid-state qubit based on spin superfluidity and spin Hall phenomena is presented. We introduce a magnetic Josephson device that realizes the spin-supercurrent analogs of the current-biased Josephson junction and the superconducting phase qubit, and show how to utilize spin Hall phenomena to perform full electrical control and readout of the qubit. We present an array of interacting magnetic phase qubits that can realize a quantum annealer. This magnetic quantum information processing device benefits from the standard solid-state materials and fabrication technology which allow for scalability. However, the upper bound for the operational temperature can, in principle, be higher than the superconducting counterpart, as it is ultimately governed by the magnetic ordering (Curie or Néel) temperatures, which could be much higher than the critical temperatures of the conventional superconducting devices.

PACS numbers: 75.45.+j, 85.75.-d, 75.78.-n, 03.67.Lx

Introduction.—Macroscopic quantum phenomena have long fascinated physicists for their importance in both fundamental science and device applications [1]. The most well-studied of the phenomena is perhaps the Josephson effect, involving dissipationless flow of electrical current between two weakly-coupled superconductors [2]. It plays a central role in superconducting Josephson devices [3], which hold promise as an architecture for a quantum bit (qubit), the basic unit of quantum information [4]. Manifestations of macroscopic quantum behavior have also been pursued in magnetic systems [5]. Indeed, macroscopic quantum phenomena have been discussed in the context of depinning of ferromagnetic domain walls [6], quantum tunneling between states with different magnetic orientations in ferromagnetic [7] and anti-ferromagnetic [8] nanoparticles, as well as molecular magnets [9]. Molecular magnets, in particular, have garnered much attention for their potential utility in quantum information technology [10]. However, an alternative macroscopic qubit in magnetic systems is yet unexplored.

In this work, we introduce the first macroscopic spin-based qubit by combining two recent advancements in the field of spintronics: spin superfluidity and spin Hall phenomena. Spin superfluidity explores how analogs of conventional superfluidity can be realized in magnetically ordered systems [11]. The conventional Josephson effect relies on macroscopic phase coherence of the two superconductors, each characterized by a U(1) order parameter. Magnetic order in certain insulating magnets are also described by macroscopic U(1) order parameters [11]. In analogy with superconductors, coupling two such magnets gives rise to the *magnetic* Josephson effect involving dissipationless (superfluid) flow of spin angular momentum between the magnets [12].

Spin Hall phenomenology is often discussed in the context of a bilayer system consisting of a normal metal with strong spin-orbit coupling and an insulating ferromagnet with well-formed magnetic order [13]. The combination of spin-orbit coupling in the metal and exchange coupling (between

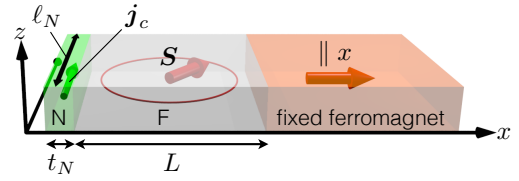


FIG. 1. Heterostructure that realizes the magnetic phase qubit. A mono-domain easy-plane ferromagnet (F), with macrospin S , is exchange-coupled to a fixed mono-domain ferromagnet (with its macrospin oriented along the x axis) and attached to a normal metal (N) with strong spin-orbit coupling. A charge current j_c is applied in the y direction in the N.

the conduction electron spins and the magnetic order) at the metal|magnet interface allow angular momentum to be transferred from the metal's crystal lattice to the ferromagnet, thus engendering macroscopic coupling between the electrical current in the metal and the magnetic moments in the ferromagnet [14]. In light of these developments, one may question whether the magnetic Josephson effect can serve as a basis for a qubit (in analogy with the superconducting Josephson devices), and whether spin Hall phenomena can realize electrical control and readout of such a qubit.

In this Letter, we show that a heterostructure consisting of magnetic insulators and a normal metal with strong spin-orbit coupling can realize a magnetic analog of the superconducting phase qubit [15] and permits full electrical control and readout via spin Hall phenomena. We refer to this device as the *magnetic phase qubit*. We show how a coupled array of these qubits can realize a quantum annealer [16], which could be used to solve certain hard optimization problems and machine learning tasks. While the electrical readout of molecular qubits can be challenging [10], spin Hall phenomena offers an alternative, and a possibly more straightforward, method for electrical control and readout of the magnetic qubit. The device is an example of a macroscopic qubit that can be constructed from state-of-the-art solid state mate-

rials and so should offer the same advantages as the superconducting qubits of strong inter-qubit coupling and scalability. However, the maximum operational temperature of the magnetic qubit can be fundamentally much higher than the superconducting devices, as it is limited by the Curie or Néel temperatures, which are much higher than the typical superconducting operating temperatures. Though the current proposal focuses on ferromagnetic systems, it is directly applicable to antiferromagnetic systems as well. As antiferromagnets can display macroscopic quantum behavior at higher temperatures than with ferromagnets [8], antiferromagnet-based qubit may be favorable than the ferromagnetic counterpart.

Model.—The prototype magnetic phase qubit consists of a ferromagnetic insulator (F) attached to a normal metal (N) with strong spin-orbit coupling and exchange-coupled to a fixed ferromagnetic layer, as shown in Fig. 1. We consider low enough temperatures such that only the lowest mode is excited in the F and it can essentially be considered in the mono-domain limit [17]. Denoting the macrospin in the F by \mathbf{S} and assuming uniaxial symmetry about the z axis, the Hamiltonian for the F can be written as

$$H = -JS_x + \frac{K}{2S} S_z^2, \quad (1)$$

where the first term arises due to the exchange coupling to the fixed ferromagnet, S_z is the z projection of \mathbf{S} , and K is the uniaxial magnetic anisotropy. Here, we assume easy-plane anisotropy with $K > 0$. The N is taken to be a metal with strong spin-orbit coupling, e.g., platinum (Pt); it is assumed to be a metallic film parallel to the yz plane obeying Ohm's law $\rho \mathbf{j}_c = \mathbf{E}$, where \mathbf{E} is the electric field, \mathbf{j}_c is the (linear) charge current density and ρ is its 2D resistivity.

Dynamics.—Well below the Curie temperature, the classical dynamics of the F macrospin (isolated from the N) is well-described by the Landau-Lifshitz-Gilbert equation

$$\hbar \dot{\mathbf{S}} = \mathbf{H}_0 \times \mathbf{S} - \frac{\hbar \alpha}{S} \mathbf{S} \times \dot{\mathbf{S}}, \quad (2)$$

where the effective field $\mathbf{H}_0 \equiv \partial H / \partial \mathbf{S}$, and the viscous damping strength is parametrized by the dimensionless Gilbert parameter α . The current in the N is used to manipulate \mathbf{S} . This is achieved by a combination of spin-orbit coupling in the N and the exchange coupling at the N|F interface between the conduction electron spins and \mathbf{S} ; they allow angular momentum to be transferred from the N crystal lattice to the F macrospin, effectively leading to a macroscopic coupling between the current and the magnetization dynamics [14]. Through this magnetoelectric coupling, the current in the N generally induces a torque $\boldsymbol{\tau}$ on \mathbf{S} , and the dynamic macrospin \mathbf{S} , in turn, induces an electromotive force $\boldsymbol{\varepsilon}$ in the N [13]. Spin Hall phenomenology allows one to write down general expressions for $\boldsymbol{\tau}$ and $\boldsymbol{\varepsilon}$ that respect certain crystalline and structural symmetries at the interface [18]. In the presence of full translational and rotational symmetries in the yz plane and with the breaking of reflection symmetry along the x axis (as we have in the current setup), spin Hall phenomenology

dictates that the torque $\boldsymbol{\tau}$ is given by

$$\boldsymbol{\tau} = \frac{\mathcal{A} \vartheta}{S^2} \mathbf{S} \times (\hat{\mathbf{x}} \times \mathbf{j}_c) \times \mathbf{S}, \quad (3)$$

where \mathcal{A} is the cross-sectional area of the interface and ϑ is the phenomenological torque coefficient for the N|F interface [19], and that the electromotive force $\boldsymbol{\varepsilon}$ takes the form

$$\boldsymbol{\varepsilon} = \frac{\vartheta}{S^2} (\mathbf{S} \times \dot{\mathbf{S}}) \times \hat{\mathbf{x}}. \quad (4)$$

The fact that the same coefficient ϑ enters both Eqs. (3) and (4) is a consequence of Onsager reciprocity [13].

The presence of the N subjects the F macrospin to additional viscous damping, which modifies the torque to $\boldsymbol{\tau} \rightarrow \boldsymbol{\tau}' \equiv \boldsymbol{\tau} - (\hbar \alpha^{\uparrow\downarrow} / S) \mathbf{S} \times \dot{\mathbf{S}}$, where $\alpha^{\uparrow\downarrow} \equiv \mathcal{A} g^{\uparrow\downarrow} / 4\pi S$ and $g^{\uparrow\downarrow}$ is the (real part of the) effective interfacial spin-mixing conductance per unit area [20]. Putting the above together, one finally arrives at the coupled dynamics of the current and the magnetization,

$$\hbar \dot{\mathbf{S}} = \mathbf{H}_0 \times \mathbf{S} - \frac{\hbar \alpha}{S} \mathbf{S} \times \dot{\mathbf{S}} + \boldsymbol{\tau}', \quad (5)$$

$$\rho \mathbf{j}_c = \mathbf{E} + \boldsymbol{\varepsilon}. \quad (6)$$

We note that the proposal can also be realized with a Heisenberg antiferromagnet (in place of the F) subjected to an external magnetic field \mathbf{B} normal to the film. Both the current model and spin Hall phenomenology directly apply to this case, but with \mathbf{S} representing the macroscopic Néel order parameter, the effective spin-mixing conductance $g^{\uparrow\downarrow}$ corresponding to the N|AF interface [11], and the field providing the anisotropy, i.e., $K \rightarrow (B/B_{\text{ex}}) \hbar \gamma_0 B$ (B_{ex} is the antiferromagnet exchange field and γ_0 is the gyromagnetic ratio).

We now focus on the magnetization dynamics Eq. (5). Assuming strong anisotropy (i.e., $K \gg J$), Eq. (5) becomes

$$\hbar \dot{S}_z = -JS \sin \varphi + j - \hbar \tilde{\alpha} S \dot{\varphi}, \quad \hbar \dot{\varphi} = \frac{K}{S} S_z + \frac{\hbar \tilde{\alpha}}{S} \dot{S}_z, \quad (7)$$

where $\tilde{\alpha} \equiv \alpha + \alpha^{\uparrow\downarrow}$ and $j \equiv \mathcal{A} \vartheta j_c$. Here, we have parametrized the macrospin via $\mathbf{S} \approx (S \cos \varphi, S \sin \varphi, S_z)$, where the linearization with respect to S_z/S is appropriate within the strong anisotropy limit. For $\tilde{\alpha} = 0$, and noticing that (φ, S_z) are conjugate variables, the effective Hamiltonian corresponding to the dynamics in Eq. (7) reads ($\eta \equiv j/JS$)

$$H_{\text{eff}} = \frac{K}{2S} S_z^2 - JS (\cos \varphi + \eta \varphi) \equiv \frac{K}{2S} S_z^2 + U(\varphi). \quad (8)$$

In this work, we assume $K/J \ll S^2$, such that the Josephson term (proportional to J) dominates in the effective Hamiltonian. Eq. (8) constitutes an important result of this work. The effective Hamiltonian has the same form as the standard current-biased Josephson junction, with the charging energy given by the anisotropy parameter K and the Josephson energy by the exchange interaction J . Here, the “bias current” j is a flow of (z -polarized) spin between the two magnets, and

is fully controllable using the external *charge* current j_c . The two macrospins with general non-parallel configurations, in fact, give rise to a flow of spin supercurrent (spin superfluidity) between the two magnets [11]. Interestingly, while the torque in Eq. (3) [which gives rise to the term proportional to η in Eq. (8)] is dissipative in the sense that it is odd under time-reversal, its effects enter the macrospin dynamics in a way still accountable by purely Hamiltonian dynamics.

Qubit.—The following results for the magnetic phase qubit can be obtained by closely following the results for the superconducting phase qubits [3, 21]. The qubit is operated at $\eta \lesssim 1$, where the “washboard” potential $U(\varphi)$ is sufficiently tilted [22]. In this regime, the potential about $\varphi = \pi/2$ can be approximated by a cubic form $U(\phi) \approx (JS - j)\phi - (JS/6)\phi^3 + \text{const.}$ (with $\phi \equiv \varphi - \pi/2$). A local minimum is located at $\phi_0 = -\sqrt{2(1-\eta)}$, and the plasma frequency corresponding to the quadratic curvature at the minimum is given by

$$\hbar\omega_p = \sqrt{KJ} [2(1-\eta)]^{1/4}. \quad (9)$$

Quantizing Eq. (8) by imposing the canonical commutation relation $[\hat{\varphi}, \hat{S}_z] = i$ leads to the quantization of energy levels inside the cubic potential, and when $\eta \lesssim 1$ only a few quantum states are bound in each of the local minima. We label the lowest three energy eigenvalues by E_0 , E_1 and E_2 , and the corresponding states by $|0\rangle$, $|1\rangle$ and $|2\rangle$. Taking account of the cubic anharmonicity to second-order in perturbation theory, the separation between the two lowest pairs of energy levels become $E_1 - E_0 \equiv \hbar\omega_{10} \approx \hbar\omega_p(1-r)$ and $E_2 - E_1 \equiv \hbar\omega_{21} \approx \hbar\omega_p(1-2r)$, where the deviations from the harmonic limit is quantified in terms of $r \equiv (5/36)(\hbar\omega_p/\Delta U)$, $\Delta U \equiv (4\sqrt{2}/3)JS(1-\eta)^{3/2}$ being the energy barrier for the particle to escape from a local minimum.

Control.—The state of the magnetic phase qubit can be controlled by introducing an ac component to j oscillating at frequency ω_{10} , i.e., $j(t) = j_{\text{dc}} + j_{\text{ac}}(t)\cos(\omega_{10}t)$, where j_{dc} is the (already considered) dc component and $j_{\text{ac}}(t)$ modulates the amplitude of the ac component. Since $j(t)$ is directly proportional to $j_c(t)$, the ac component to j can be introduced simply by adding an ac component to the charge current. To inhibit transitions between states $|1\rangle$ and $|2\rangle$, one requires the temporal variations of $j_{\text{ac}}(t)$ to be slow compared to $2\pi/(\omega_{21} - \omega_{10})$. In this limit, and for temperatures $T \ll \hbar\omega_{10}/k_B$, the Hilbert space for the qubit is spanned by the two lowest states $|0\rangle$ and $|1\rangle$, and the effective Hamiltonian reads

$$\hat{H}_{\text{eff}} = -\frac{\hbar\omega_{10}}{2}\hat{\sigma}^z - \frac{j_{\text{ac}}(t)\gamma}{2} \begin{pmatrix} 0 & e^{i\omega_{10}t} \\ e^{-i\omega_{10}t} & 0 \end{pmatrix}, \quad (10)$$

where $\gamma \equiv \sqrt{K/2S\hbar\omega_{10}}$ and we have invoked the rotating wave approximation and the off-diagonal elements were computed using harmonic oscillator states due to the small non-linearity of the system. The qubit can undergo Rabi oscillations, where the probability for transition between $|0\rangle$ and $|1\rangle$ states $P_{0 \rightarrow 1}(t) = \sin^2[\Omega_{\text{ac}}(t)t]$, where $\hbar\Omega_{\text{ac}}(t) \equiv j_{\text{ac}}(t)\gamma/2$. The application of an ac pulse over time interval $\Delta t = \pi/2\Omega_{\text{ac}} \equiv t_0$ drives the qubit from state $|0\rangle$ to $|1\rangle$. With a pulse of length

$\Delta t = t_0/2$, the qubit can be manipulated into the superposition state $(|0\rangle + |1\rangle)/\sqrt{2}$.

Read out.—The state of the qubit can be read out by adiabatically lowering the potential barrier ΔU close to E_1 such that the qubit in state $|1\rangle$ is (exponentially) more likely to tunnel out of a local minimum than that in state $|0\rangle$. The limit $\Delta U \rightarrow E_1$ is achieved as $\eta \rightarrow 1$. Once the “particle” tunnels out of the local minimum, it will descend down the washboard potential and a finite $\langle\dot{\varphi}\rangle$ results. According to Eq. (4), a finite $\langle\dot{\varphi}\rangle$ generates an electromotive force $\mathcal{E} \approx \partial\langle\dot{\varphi}\rangle/\partial t$ [23], so that Ohm’s law in the N is modified to $(\rho - \delta\rho)j_c = E$. We can estimate $\delta\rho$ by considering the motion of the particle classically. Approximating the washboard potential as a downward-sloping line connecting all of the local minima, the descending particle (damped by Gilbert damping $\tilde{\alpha}$) will reach a terminal velocity $\dot{\varphi}_t = \mathcal{A}\partial j_c/\partial\tilde{\alpha}S$. The correction to the effective resistivity thus reads $\delta\rho = \mathcal{A}\partial^2/\partial\tilde{\alpha}S$. For a fixed j_c , $\delta\rho$ gives rise to a decrease in voltage of $\delta V = \delta\rho j_c \ell_N$ across the N, where ℓ_N is the length of the N in the y direction. The tunneling out of state $|1\rangle$ can be detected by detecting this voltage decrease. To detect state $|0\rangle$, one may transfer the qubit to state $|1\rangle$ using a resonant ac pulse, and then detect state $|1\rangle$.

Decoherence.—Decoherence in the magnetic phase qubit arises from various environmental degrees of freedom that couple to the macrospin, e.g., the phonons in the F as well as the electron continuum in the N. Dissipation due to these environments have been accounted for by Gilbert damping. A damped macrospin experiences a stochastic force required to exist by the fluctuation-dissipation theorem [24]. The stochastic force can be described by introducing a random component, $\delta H_{\text{eff}}(t) = h_\varphi(t)\varphi + h_{S_z}(t)S_z$, to the effective classical Hamiltonian (8), where $h_\varphi(t)$ and $h_{S_z}(t)$ are the stochastic fields. Quantizing Eq. (8) in the presence of the stochastic fields and projecting the result to the two lowest quantum states, the effective quantum Hamiltonian (10) also becomes endowed by an additional stochastic contribution $\delta\hat{H}_{\text{eff}}(t) = \tilde{h}_x(t)\hat{\sigma}^x + \tilde{h}_y(t)\hat{\sigma}^y$, where the new stochastic fields obey

$$\langle\tilde{h}_x(\omega)\tilde{h}_x(\omega')\rangle = \frac{\hbar\tilde{\alpha}K}{2} \frac{\omega}{\omega_{10}} \coth\left(\frac{\hbar\omega}{2k_B T}\right) (2\pi)\delta(\omega + \omega') \quad (11)$$

$$\text{and } \langle\tilde{h}_y(\omega)\tilde{h}_y(\omega')\rangle = (\hbar\omega_{10}/K)^2 \langle\tilde{h}_x(\omega)\tilde{h}_x(\omega')\rangle.$$

To discuss the effects of decoherence, we consider the qubit in the absence of the ac drive, i.e., $j_{\text{ac}}(t) = 0$. Decoherence is characterized by the longitudinal relaxation rate $\Gamma_1 = 1/T_1$ and the dephasing rate $\Gamma_2 = 1/T_2$. Using Fermi’s golden rule, Γ_1 due to the stochastic fields reads [21, 25]

$$\Gamma_1 \approx \frac{\tilde{\alpha}K}{2\hbar}, \quad (12)$$

where the approximation holds in the strong anisotropy limit, $K \gg J$ (assumed in this work), and in the low temperature regime, $k_B T \ll \hbar\omega_{10}$ [26]. Since the stochastic fields only involve transverse components, the dephasing rate is simply related to the relaxation rate through $\Gamma_2 = \Gamma_1/2$.

Qubit coupling.—Let us consider an array of identical magnetic phase qubits as shown in Fig. 2. Every qubit is coupled

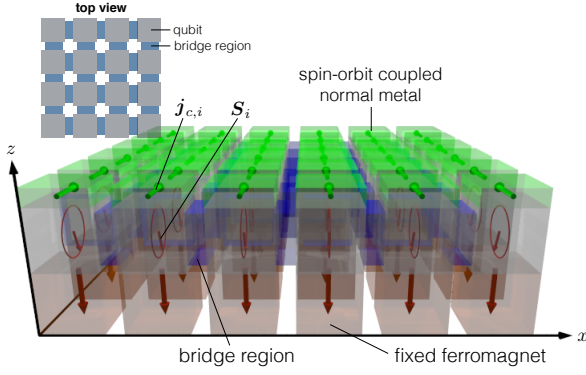


FIG. 2. A coupled array of magnetic phase qubits realizing a quantum annealer. Each qubit is coupled to its own normal metal with independently tunable dc and ac currents. The bridge regions (shaded in blue) mediate exchange coupling between nearest neighbor ferromagnets and give rise to effective inter-qubit coupling.

to its own N so that its splitting $\hbar\omega_{10,i}$ and the Rabi frequency $\Omega_{ac,i}$ can be tuned independently by adjusting the dc and ac amplitudes of $j_{c,i}(t)$, respectively (i here labels the qubits). We connect neighboring Fs via a “bridge” (shaded in blue), which is also an insulating ferromagnet and mediates an exchange interaction J'_{ij} between i -th and j -th Fs. The coupling J'_{ij} can be tuned by adjusting the cross-sectional area of each bridge, a narrower (wider) bridge leading to a relatively weak (strong) coupling. Again for strong easy-plane anisotropy ($K \gg J'_{ij}$), the interaction becomes $H_{\text{int}} \approx -\sum_{\langle i,j \rangle} J'_{ij} S \cos(\varphi_i - \varphi_j)$, where $\langle i,j \rangle$ label the nearest neighbor qubits. Quantizing this Hamiltonian and projecting it to the two lowest states of each qubit, the interaction Hamiltonian reads [27]

$$\hat{H}_{\text{int}} = \sum_{\langle i,j \rangle} J'_{ij} \gamma^2 S \hat{\sigma}_i^x \hat{\sigma}_j^x. \quad (13)$$

The coupled array of qubits is then described by the total Hamiltonian $\hat{H}_t = \hat{H}_0 + \hat{H}_{\text{int}}$, where

$$\hat{H}_0 = - \sum_i \left[\frac{\hbar\omega_{10,i}}{2} \hat{\sigma}_i^z + \frac{j_{ac,i}\gamma}{2} \begin{pmatrix} 0 & e^{i\omega_{10,i}t} \\ e^{-i\omega_{10,i}t} & 0 \end{pmatrix} \right]. \quad (14)$$

Quantum annealer.—A quantum annealer solves hard optimization problems by finding the ground state of a “problem Hamiltonian” through a process involving quantum fluctuations. It can be implemented with a classical Ising Hamiltonian that encodes the computational problem, and a transverse field term, $\hat{H}_{\text{QA}}(t) = -A(t) \sum_i \hat{\sigma}_i^x + B(t) \hat{H}_{\text{Ising}}$, where $\hat{H}_{\text{Ising}} = -\sum_i h_i \hat{\sigma}_i^z - \sum_{i,j} J_{ij} \hat{\sigma}_i^z \hat{\sigma}_j^z$, i, j label lattice sites, and t runs from 0 to t_f . At $t = 0$ (and temperature T), the quantum annealing process begins in the limit of strong transverse field, i.e., $A(0) \gg \{k_B T, |B(0)h_i|, |B(0)J_{ij}|\} \forall i, j$, when the quantum-mechanical fluctuations dominate, and then one gradually decreases $A(t)$ and increases $B(t)$ such that the state of system approaches a classical bit string that ideally representing the ground state of the problem Hamiltonian. Generally, at sufficiently low temperatures, the quality of solution is improved

$\hbar\omega_{10}/k_B$	$T_1 = T_2/2$	τ_{2q}/T_1	$ \delta V $
100mK	10 μ s	10 $^{-4}$	1V

TABLE I. Table summarizing the main parameters of the magnetic phase qubit. The qubit splitting and the two-qubit time scale are denoted by $\hbar\omega_{10}$ and τ_{2q} , respectively, and δV is the voltage generated during the readout process across $\ell_N = 1\mu\text{m}$ length of the N.

when time-scale of annealing schedule is substantially larger than the inverse of the square of the minimum gap between instantaneous ground-state and the first excited state of the effective many-body Hamiltonian given by \hat{H}_{QA} . Rotating the spin axes of all the qubits by $\pi/2$ about the y axis (such that $\hat{\sigma}_{z,x} \rightarrow \pm \hat{\sigma}_{x,z}$), \hat{H}_t can be shown to mimic the Hamiltonian \hat{H}_{QA} so the coupled array of magnetic phase qubits above can be used to implement quantum annealing.

Discussion.—The qubit must operate at temperatures $k_B T \ll \hbar\omega_{10} \equiv k_B T_+ \sim \sqrt{KJ}$ [c.f. Eq. (9)] [28]. Here, we take both the F and the fixed ferromagnet to be $1\mu\text{m} \times 1\mu\text{m} \times 0.1\mu\text{m}$ films of yttrium iron garnet (YIG), an insulating ferrimagnet. Assuming the easy-plane to be the film plane (arising due to shape anisotropy), modeling YIG as a cubic crystal ($a = 12\text{\AA}$) with effective $S_0 = 14.2$ [29], and using $J/K \sim 0.1$, we find $T_+ \approx 100\text{mK}$ (comparable to the superconducting phase qubits [15]). Using $\alpha \sim 10^{-5}$ (for YIG) [30], and assuming that the damping enhancement $\alpha^{\uparrow\downarrow}$ due to the N just exceeds α , we take $\tilde{\alpha} \sim 10^{-5}$. We then obtain $T_1 \sim 10\mu\text{s}$. As shown above, the non-linearity necessary for the qubit to remain within the two-level subspace requires $\eta \sim 1$. The (linear) current density necessary to achieve this is $\bar{j}_c \sim JS/\mathcal{A}\vartheta$. Here, $\vartheta = \hbar \tan \theta_{\text{SH}}/2et_N$, where θ_{SH} is the effective spin Hall angle for the N/F interface and t_N is the N thickness [18]. Using $\theta_{\text{SH}} \sim 0.1$ (appropriate for Pt|YIG interface), $t_N = 10\text{nm}$, and setting all other parameters to the values above, we obtain $\bar{j}_c \sim 10^6 \text{A} \cdot \text{m}^{-1}$. Based on the same parameters (and using $j_c \sim 10^6 \text{A} \cdot \text{m}^{-1}$), the magnitude of the voltage decrease that needs to be detected for the readout process is $\delta V \sim 1\text{V}$. Finally, from Eq. (13), the ratio of the two-qubit time scale τ_{2q} to T_1 time can be estimated as $\tau_{2q}/T_1 = \tilde{\alpha}\hbar\omega_{10}/J'_{ij} \sim \tilde{\alpha}(KJ)^{1/2}/J'_{ij}$. Taking $J'_{ij} \sim J$ (and again assuming $J/K \sim 0.1$ and $\tilde{\alpha} \sim 10^{-5}$), we obtain $\tau_{2q}/T_1 \sim 10^{-4}$. The important parameters are summarized in Table I [31].

To reduce the Joule heating caused by the current in the N, one may reduce J in order to decrease \bar{j}_c . However, a decrease in J will also lead to an undesirable decrease in T_+ . Alternatively, \bar{j}_c can be reduced, with possibly little effect on T_+ , by increasing the effective spin Hall angle θ_{SH} ; this may be achieved by using materials with strong effective spin Hall angles like topological insulators in place for the N [32]. An increase in K together with a decrease in $\tilde{\alpha}$ is also desirable in order to increase T_+ without compromising the $T_{1,2}$ times.

Summary and outlook.—We propose a solid-state device that can prepare and control macroscopic quantum states by utilizing the physics of the spin superfluidity and spin Hall phenomena. This spin-supercurrent device can be used for

preparing macroscopic quantum entanglement, probabilistic information processing, quantum annealing and quantum-assisted sensing in analogy with the corresponding superconducting devices including the current-biased Josephson qubits, superconducting quantum annealers and the SQUID magnetometers. Our estimation of the relevant physical parameters based on the state-of-the-art technology shows similar range of operating temperatures, single- and two-qubit energy scales, and relaxation time scales as the existing superconducting electronics. However, our proposed spintronic device might be eventually more energy efficient and robust since its operating temperature is bounded by the magnetic ordering (Curie or Néel) temperatures, which could, in principle, be much higher than the superconducting transition temperatures.

Acknowledgments.—S. T. would like to thank Pramey Upadhyaya for discussions. This work was supported by FAME (an SRC STARnet center sponsored by MARCO and DARPA).

APPENDIX A: DECOHERENCE MODEL

In this section, we derive Eqs. (11) and (12). The stochastic component to the classical effective Hamiltonian $\delta H_{\text{eff}}(t)$ (defined in the main text) modifies Eq. (10) to

$$\begin{aligned} \hbar \dot{S}_z &= -JS \sin \varphi + j - \hbar \tilde{\alpha} S \dot{\varphi} - h_\varphi, \\ \hbar \dot{\varphi} &= \frac{K}{S} S_z + \frac{\hbar \tilde{\alpha}}{S} \dot{S}_z + h_{S_z}. \end{aligned} \quad (\text{A.1})$$

By fluctuation-dissipation theorem, the correlators for the stochastic fields then read [24]

$$\begin{aligned} \langle h_\varphi(\omega) h_\varphi(\omega') \rangle &= S^2 \chi(\omega) (2\pi) \delta(\omega + \omega'), \\ \langle h_{S_z}(\omega) h_{S_z}(\omega') \rangle &= \chi(\omega) (2\pi) \delta(\omega + \omega'), \end{aligned} \quad (\text{A.2})$$

where $\chi(\omega) = (\hbar^2 \tilde{\alpha} \omega / S) \coth(\hbar \omega / 2k_B T)$. We now promote both φ and S_z to quantum-mechanical operators, and project $\delta H_{\text{eff}}(t)$ to the two lowest quantum states $|0\rangle$ and $|1\rangle$. If the states are approximated as harmonic oscillator states (as done in the main text) [21], we have

$$\langle 0 | \hat{\varphi} | 1 \rangle \approx \gamma, \quad \langle 0 | \hat{S}_z | 1 \rangle \approx -\frac{i}{2\gamma}, \quad (\text{A.3})$$

and the diagonal elements vanish. The stochastic contribution to the two-level Hamiltonian then becomes $\delta \hat{H}_{\text{eff}}(t) = \tilde{h}_x(t) \hat{\sigma}^x + \tilde{h}_y(t) \hat{\sigma}^y$ (as introduced in the main text), with $\tilde{h}_x(t) = \gamma h_\varphi(t)$ and $\tilde{h}_y(t) = (2\gamma)^{-1} h_{S_z}(t)$. Here, the noise correlators are given by $\langle \tilde{h}_x(\omega) \tilde{h}_x(\omega') \rangle = \gamma^2 \langle h_\varphi(\omega) h_\varphi(\omega') \rangle$ and $\langle \tilde{h}_y(\omega) \tilde{h}_y(\omega') \rangle = (2\gamma^2 S)^{-2} \langle h_{S_z}(\omega) h_{S_z}(\omega') \rangle$, which gives Eq. (11).

To estimate the T_1 and T_2 times, we consider the undriven qubit, i.e., $j_{\text{ac}}(t) = 0$. In the limit of strong anisotropy (i.e., $K \gg J$) we have $2\gamma^2 S \gg 1$, so we may ignore the fluctuations $\tilde{h}_y(t)$ in this estimate. The relevant two-level Hamiltonian then reads

$$\hat{H}_{\text{eff}} \approx -\frac{\hbar \omega_{10}}{2} \hat{\sigma}_z + \tilde{h}_x(t) \hat{\sigma}_x. \quad (\text{A.4})$$

The second term in Eq. (A.4) causes transitions between the two qubit states. If the qubit starts in state $|1\rangle$ at $t = 0$, the amplitude for the qubit to be in the ground state $|0\rangle$ at time t is given by (using Fermi's golden rule)

$$c_0(t) \approx \frac{1}{i\hbar} \int_0^t dt' \langle 0 | \tilde{h}_x(t) \hat{\sigma}_x | 1 \rangle e^{i\omega_{10}t'}. \quad (\text{A.5})$$

Then the noise-averaged probability $p_0(t) \equiv \langle |c_0(t)|^2 \rangle$ reads

$$\begin{aligned} p_0(t) &= \frac{1}{\hbar^2} \int_0^t \int_0^t dt' dt'' \langle \tilde{h}_x(t') \tilde{h}_x(t'') \rangle e^{i\omega_{10}(t'-t'')} \\ &= \frac{\gamma^2 S^2}{\hbar^2} \int \frac{d\omega}{2\pi} \frac{\sin^2\left(\frac{\omega - \omega_{10}}{2} t\right)}{\left(\frac{\omega - \omega_{10}}{2}\right)^2} \chi(\omega). \end{aligned} \quad (\text{A.6})$$

Most of the integral contribution in Eq. (A.6) comes from $\omega \sim \omega_{10}$. In the quantum regime (i.e., $\hbar \omega_{10} \gg k_B T$), $\chi(\omega)$ is a slow-varying function of ω while its pre-factor inside the integrand is strongly peaked at $\omega = \omega_{10}$. Then the integral can be approximated by evaluating $\chi(\omega)$ at $\omega = \omega_{10}$ and taking it out of the integral. The probability is then given by

$$p_0(t) \approx \frac{\gamma^2 S^2 \chi(\omega_{10})}{\hbar^2} t = \frac{\tilde{\alpha} K}{2\hbar} t, \quad (\text{A.7})$$

which leads to the longitudinal relaxation rate $\Gamma_1 = \dot{p}_0$ in Eq. (12).

APPENDIX B: ESTIMATING MAGNETIC PHASE QUBIT PARAMETERS

In this section, we provide more details on the numerical estimates presented in the *Discussion* section. The magnetic anisotropy parameter K for the F was determined as follows. We assume that the anisotropy purely arises from the shape anisotropy. For a thin film, the shape anisotropy energy per unit volume is given by

$$e_{\text{an}} = \frac{1}{2} \mu_0 M_s^2 \cos^2 \theta, \quad (\text{B.1})$$

where μ_0 is the magnetic permeability, M_s is the saturation magnetization per unit volume, and θ is the angle the magnetization subtends to the plane normal. Since the macrospin magnitude for the F is S (in units of \hbar), we have $M_s = \gamma_0 \hbar S / \mathcal{V}$, where γ_0 is the gyromagnetic ratio and \mathcal{V} is the volume of the F. Inserting this into Eq. (B.1), we obtain the total anisotropy energy (integrated over the volume)

$$e_{\text{an}} = \frac{1}{2} \frac{\mu_0 \gamma_0^2 \hbar^2}{\mathcal{V}} S_z^2. \quad (\text{B.2})$$

Comparing this with Eq. (1), we obtain

$$K = \frac{\mu_0 \gamma_0^2 S}{\mathcal{V}}. \quad (\text{B.3})$$

Since $S = S_0 \mathcal{V} / a^3$ (and using $\mu_0 = 1.257 \times 10^{-6} \text{ T}\cdot\text{m}\cdot\text{A}^{-1}$ and $\gamma_0 = 1.76 \times 10^{11} \text{ s}^{-1}\cdot\text{T}^{-1}$), we have $K \approx 3.56 \times 10^{-24} \text{ J}$. Using this value for K , $\Gamma_1 \approx 1.69 \times 10^5 \text{ s}^{-1}$.

The qubit non-linearity leads to the deviations of the energy levels from the harmonic oscillator levels. The deviations are necessary for the qubit to operate within the two-lowest states, and are parametrized in the main text by the variable r . For the qubit to operate in the non-linear regime, r must be of order 1. This means

$$r = \frac{5}{36} \frac{\hbar \omega_p}{\Delta U} \approx 0.08 \sqrt{\frac{K}{J}} \frac{1}{S(1-\eta)^{5/4}} \sim 1. \quad (\text{B.4})$$

Since $S \gg 1$ [and $0.08(K/J)^{1/2} \sim \mathcal{O}(1)$], the above implies that $\eta \sim 1$. This is achieved when $\vartheta \mathcal{A} j_c / JS \sim 1$, which leads to the expression for the critical current density \bar{j}_c .

-
- [1] A. Caldeira and A. Leggett, *Annals of Physics* **149**, 374 (1983).
[2] B. D. Josephson, *Phys. Lett.* **1**, 251 (1962).
[3] A. Zagoskin and A. Blais, *Phys. Can.* **63**, 215 (2007).
[4] M. A. Nielsen and I. L. Chuang, *Quantum Computation and Quantum Information* (Cambridge University Press, Cambridge, 2000).
[5] L. Gunther and B. Barbara, eds., *Quantum Tunneling of Magnetization* (Springer, 1995); E. M. Chudnovsky and J. Tejada, *Macroscopic Quantum Tunneling of the Magnetic Moment* (Cambridge University Press, 1998).
[6] T. Egami, *Phys. Status Solidi* (a) **20**, 157 (1973); *Phys. Status Solidi* (b) **57**, 211 (1973); P. C. E. Stamp, *Phys. Rev. Lett.* **66**, 2802 (1991); E. M. Chudnovsky, O. Iglesias, and P. C. E. Stamp, *Phys. Rev. B* **46**, 5392 (1992); G. Tatara and H. Fukuyama, *Phys. Rev. Lett.* **72**, 772 (1994); H.-B. Braun and D. Loss, *Phys. Rev. B* **53**, 3237 (1996); H.-B. Braun, J. Kyriakidis, and D. Loss, *Phys. Rev. B* **56**, 8129 (1997); K. Hong and N. Giordano, *J. Phys.: Condens. Matter* **8**, L301 (1996); J. Brooke, T. F. Rosenbaum, and G. Aeppli, *Nature* **413**, 610 (2001).
[7] E. M. Chudnovsky and L. Gunther, *Phys. Rev. Lett.* **60**, 661 (1988); C. Paulsen, L. C. Sampaio, B. Barbara, R. Tucoulou-Tachoueres, D. Fruchart, A. Marchand, J. L. Tholence, and M. Uehara, *Europhys. Lett.* **19**, 643 (1992).
[8] B. Barbara and E. M. Chudnovsky, *Phys. Lett. A* **145**, 205 (1990); I. V. Krive and O. B. Zaslavskii, *J. Phys.: Condens. Matter* **2**, 9457 (1990); D. D. Awschalom, J. F. Smyth, G. Grinstein, D. P. DiVincenzo, and D. Loss, *Phys. Rev. Lett.* **68**, 3092 (1992); D. D. Awschalom, D. P. DiVincenzo, and J. F. Smyth, *Science* **258**, 414 (1992); S. Gider, D. Awschalom, T. Douglas, S. Mann, and M. Chaparala, *Phys. Rev. Lett.* **76**, 3830 (1996); L. Thomas, F. Lioni, R. Ballou, D. Gatteschi, R. Sessoli, and B. Barbara, *Nature* **383**, 145 (1996); B. Barbara, L. Thomas, F. Lioni, I. Chiorescu, and A. Sulpice, *J. Magn. Magn. Mat.* **200**, 167 (1999); W. Wernsdorfer and R. Sessoli, *Science* **284**, 133 (1999).
[9] A. Chiolero and D. Loss, *Phys. Rev. Lett.* **80**, 169 (1998); F. Meier and D. Loss, *Phys. Rev. B* **64**, 224411 (2001); J. R. Friedman, M. P. Sarachik, J. Tejada, and R. Ziolo, *Phys. Rev. Lett.* **76**, 3830 (1996); L. Thomas, F. Lioni, R. Ballou, D. Gatteschi, R. Sessoli, and B. Barbara, *Nature* **383**, 145 (1996); B. Barbara, L. Thomas, F. Lioni, I. Chiorescu, and A. Sulpice, *J. Magn. Magn. Mat.* **200**, 167 (1999); W. Wernsdorfer and R. Sessoli, *Science* **284**, 133 (1999).
[10] M. N. Leuenberger and D. Loss, *Nature* **410**, 789 (2001); J. Tejada, E. M. Chudnovsky, E. del Barco, J. M. Hernandez, and T. P. Spiller, *Nanotechnology* **12**, 181 (2001); F. Meier, J. Levy, and D. Loss, *Phys. Rev. Lett.* **90**, 047901 (2003); *Phys. Rev. B* **68**, 134417 (2003); D. Rugar, R. Budakian, H. J. Mamin, and B. W. Chui, *Nature* **430**, 329 (2004); J. Lehmann, A. Gaita-Arino, E. Coronado, and D. Loss, *Nature Nano.* **2**, 312 (2007); C. J. Wedge, G. A. Timco, E. T. Spielberg, R. E. George, F. Tuna, S. Rigby, E. J. L. McInnes, R. E. P. Winpenny, S. J. Blundell, and A. Ardavan, *Phys. Rev. Lett.* **108**, 107204 (2012).
[11] E. B. Sonin, *Adv. Phys.* **59**, 181 (2010); S. Takei and Y. Tserkovnyak, *Phys. Rev. Lett.* **112**, 227201 (2014); W. Chen and M. Sigrist, *Phys. Rev. B* **90**, 094408 (2014); W. Chen and M. Sigrist, *Phys. Rev. B* **89**, 024511 (2014).
[12] A. Schilling and H. Grundmann, *Ann. Phys.* **327**, 2301 (2012).
[13] A. Brataas, Y. Tserkovnyak, G. E. W. Bauer, and P. J. Kelly, in *Spin Currents*, edited by S. Maekawa, S. O. Valenzuela, E. Saitoh, and T. Kimura (Oxford University Press, Oxford, 2012) pp. 87–135, arXiv:1108.0385.
[14] Y. Kajiwar, K. Harii, S. Takahashi, J. Ohe, K. Uchida, M. Mizuguchi, H. Umezawa, H. Kawai, K. Ando, K. Takanashi, S. Maekawa, and E. Saitoh, *Nature* **464**, 262 (2010); C. W. Sandweg, Y. Kajiwar, A. V. Chumak, A. A. Serga, V. I. Vasyuchka, M. B. Jungfleisch, E. Saitoh, and B. Hillebrands, *Phys. Rev. Lett.* **106**, 216601 (2011); C. Burrowes, B. Heinrich, B. Kardasz, E. A. Montoya, E. Girt, Y. Sun, Y.-Y. Song, and M. Wu, *Appl. Phys. Lett.* **100**, 092403 (2012); C. Hahn, G. de Loubens, O. Klein, M. Viret, V. V. Naletov, and J. Ben Youssef, *Phys. Rev. B* **87**, 174417 (2013); L. J. Cornelissen, J. Liu, R. A. Duine, J. B. Youssef, and B. J. van Wees, *Nature Phys.* **11**, 1022 (2015).
[15] J. Martinis, *Quantum Information Processing*, **8**, 81 (2009).
[16] T. Kadowaki and H. Nishimori, *Phys. Rev. E* **58**, 5355 (1998).
[17] Within the exchange approximation, a thermal magnon mode in the F with wavenumber \mathbf{mq} obeys a linear sound-like dispersion $\omega_{\mathbf{mq}} = v|\mathbf{mq}|$, where $v = \sqrt{AK\mathcal{V}}/\hbar$ is the magnon velocity, and A and \mathcal{V} are the exchange stiffness and volume of the F, respectively. The temperature constraint for mono-domain operation then translates to $T \ll \hbar v \pi / k_B L$, where L is the linear dimension of the F.
[18] Y. Tserkovnyak and S. A. Bender, *Phys. Rev. B* **90**, 014428 (2014).
[19] In addition to the so-called dissipative torque expressed in Eq. (3), symmetry generally allows another torque term, the so-called reactive torque, which is proportional to $(\hat{\mathbf{m}} \times \mathbf{m} \cdot \mathbf{j}) \times \mathbf{m} S$. For diffusive metals (like the normal metals considered here), the coefficient for the reactive term is expected to be much smaller than that of the dissipative term; we therefore neglect the reactive torque contribution in this work.
[20] Strictly speaking, this relation between $\alpha^{\uparrow\downarrow}$ and $g^{\uparrow\downarrow}$ holds if the N is a perfect spin sink. Pt and Ta are indeed good spin sinks.
[21] J. M. Martinis, S. Nam, J. Aumentado, K. M. Lang, and C. Urbina, *Phys. Rev. B* **67**, 094510 (2003).
[22] Here, we do not consider $\eta > 1$ since the potential does not possess local minima in this regime.
[23] Here, we retain only the y component of the electromotive force, as the z component is counteracted by an electrostatic buildup along the z axis (supposing the magnetic dynamics are slow compared to the relevant RC time of the normal metal).
[24] L. D. Landau and E. M. Lifshitz, *Statistical Physics, Part 1*, 3rd ed., Course of Theoretical Physics, Vol. 5 (Pergamon, Oxford, 1980).
[25] G. Ithier, E. Collin, P. Joyez, P. J. Meeson, D. Vion, D. Esteve, F. Chiarello, A. Shnirman, Y. Makhlin, J. Schrieffer, and

- G. Schön, Phys. Rev. B **72**, 134519 (2005).
- [26] See Supplementary Material for details on the results of this section.
- [27] The exchange interaction H_{int} also gives rise to terms of order J'/J that renormalize the qubit frequency $\hbar\omega_{10}$; we neglect this correction as it is not essential to the following discussion.
- [28] At these temperatures, the system is well-within the regime for mono-domain operation, for T_+ is set by \sqrt{KJ} , where $J \ll K$ (by assumption here), while the upper bound for mono-domain operation is set by $\sqrt{KJ_{\text{ex}}}$, where J_{ex} is the exchange interaction between the spins within the F, and typically $J_{\text{ex}} \gg K$.
- [29] M. A. Gilleo and S. Geller, Phys. Rev. **110**, 73 (1958).
- [30] S. Bhagat, H. Lessoff, C. Vittoria, and C. Guenzer, Phys. Status Solidi **20**, 731 (1973).
- [31] Further details on these numerical estimates are included in the Supplementary Material.
- [32] Y. Fan, P. Upadhyaya, X. Kou, M. Lang, S. Takei, Z. Wang, J. Tang, L. He, L.-T. Chang, M. Montazeri, G. Yu, W. Jiang, T. Nie, R. N. Schwartz, Y. Tserkovnyak, and K. L. Wang, Nature Mater. **13**, 699 (2014).